

FLUTE: Fast Lookup Table Based Rectilinear Steiner Minimal Tree Algorithm for VLSI Design

Chris Chu and Yiu-Chung Wong

Abstract—In this paper, we present a very fast and accurate rectilinear Steiner minimal tree (RSMT) algorithm called FLUTE. FLUTE is based on pre-computed lookup table to make RSMT construction very fast and very accurate for low-degree¹ nets. For high-degree nets, a net breaking technique is proposed to reduce the net size until the table can be used. A scheme is also presented to allow users to control the tradeoff between accuracy and runtime.

FLUTE is optimal for low-degree nets (up to degree 9 in our current implementation) and is still very accurate for nets up to degree 100. So it is particularly suitable for VLSI applications in which most nets have a degree 30 or less. We show experimentally that over 18 industrial circuits in the ISPD98 benchmark suite, FLUTE with default accuracy is more accurate than the Batched 1-Steiner heuristic and is almost as fast as a very efficient implementation of Prim's rectilinear minimum spanning tree (RMST) algorithm.

Index Terms—Rectilinear Steiner Minimal Tree Algorithm, Wirelength Estimation, Wirelength Minimization, Routing, Interconnect Optimization

I. INTRODUCTION

A rectilinear Steiner minimal tree (RSMT) is a tree with minimum total edge length in Manhattan distance to connect a given set of nodes possibly through some extra (i.e., Steiner) nodes. RSMT construction is a fundamental problem that has many applications in VLSI design. In early design stages like physical synthesis, floorplanning, interconnect planning and placement, it can be used to estimate wireload, routing congestion and interconnect delay. In global and detailed routing stages, it is used to generate the routing topology of each net.

RSMT problem is NP-complete [1]. So, in practice, rectilinear minimum spanning tree (RMST) is often used instead of RSMT. This approach is particularly common in early design stages in which the design space is being explored and hence a fast tree construction algorithm is crucial. The disadvantage of this approach is that the length of RMST may be much longer than that of RSMT since Steiner node is not allowed. Hwang [2] showed that length of RMST can be as much as 1.5 times that of RSMT. However, the difference is typically far less than 50% in practice. So this inaccuracy is tolerable in early design stages.

Chris Chu is with the Department of Electrical and Computer Engineering, Iowa State University, Ames, IA 50010 (email: cnchu@iastate.edu).

Yiu-Chung Wong is with Rio Design Automation, Santa Clara, CA 95054 (email: ycwong@rio-da.com).

¹The degree of a net is the number of pins in the net.

At later stages in which better wirelength is required, RSMT construction is necessary. Hwang et al. [3] provided a comprehensive discussion of various RSMT algorithms. For optimal RSMT algorithm, the fastest implementation is currently the GeoSteiner package [4], [5]. Griffith et al. [6] (Batched 1-Steiner heuristic) and Mandoiu et al. [7] are two well-known near-optimal algorithms. However, these optimal and near-optimal algorithms are computationally too expensive to be used in VLSI design applications.

Many attempts have been made to design RSMT algorithms with lower runtime complexity. Borah et al. [8] presented an $O(n^2)$ time algorithm in which a spanning tree is iteratively improved by connecting a point to a nearby edge and deleting the longest edge on the created cycle. An $O(n \log n)$ time but very complicated alternative implementation was also proposed. Zhou [9] used spanning graph [10] to help both generating the initial spanning tree and finding good candidates for the edge substitution idea in [8]. The resulting algorithm runs in $O(n \log n)$ time, and produces better solution in slightly less runtime than the one in [8]. Kahng et al. [11] gave a practical $O(n \log^2 n)$ heuristic called BGA based on a batched version of the greedy triple contraction algorithm. This algorithm produces a better solution quality and requires a slightly shorter runtime than [8] and [9] in practice.

Most signal nets in VLSI circuits have a low degree. So in VLSI applications, rather than having a low runtime complexity, it is more important for RSMT algorithms to be simple so that it can be efficient for small nets. An example of such an approach is the single trunk Steiner tree (STST), which is constructed by connecting each pin to a trunk that goes either horizontally or vertically through the median position of all pins [12]. However, the length of STST is far from optimal even for medium size nets (e.g., degree 10–15). Hence its application is limited. Chen et al. [13] proposed an algorithm called Refined Single Trunk Tree (RST-T) to reduce the length of STST by a refining procedure. RST-T is proved to be optimal for nets up to degree 4 and is experimentally shown to be optimal for degree 5 nets. It is reasonably accurate for medium size nets too. RST-T runs in $O(n \log n)$ time with a fairly small constant.

In this paper, we present a very fast and accurate lookup table based RSMT algorithm called FLUTE. We show that the set of all degree- n nets can be partitioned into $n!$ groups according to the relative positions of their pins. For each group, the optimal wirelength of any net can be found based on a few vectors called *potentially optimal wirelength vectors* (POWVs). Each POWV corresponds to a linear combination of distances between adjacent pins. We pre-compute the few POWVs for each group and store them into a table. Associated

with each POWV, we also store one corresponding Steiner tree, which we called *potentially optimal Steiner tree* (POST). To find the optimal RSMT of a net, we just need to compute the wirelengths corresponding to the POWVs for the group the net belongs to, and then return the POST associated with the POWV with minimum wirelength. This lookup table idea can optimally and efficiently handle low-degree nets (up to degree 9 in our implementation). For high-degree nets, we proposed a net breaking technique to recursively break a net until the table can be used. A scheme is also presented to allow users to control the tradeoff between accuracy and runtime during net breaking. The runtime complexity of FLUTE with fixed accuracy is $O(n \log n)$ for a net of degree n .

Since FLUTE is extremely fast and accurate for low-degree nets, it is especially suitable for VLSI applications. We show experimentally that over 18 industrial circuits in the ISPD98 benchmark suite [14], FLUTE with default accuracy is more accurate than the Batched 1-Steiner heuristic [6] and is almost as fast as a very efficient implementation of Prim's RMST algorithm [15]. By adjusting the accuracy parameter, the error can be further reduced with only a small increase in runtime (e.g., $3.1\times$ error reduction with $2.0\times$ runtime increase). In addition, we show that even for high-degree nets (up to degree 100), it is still very fast and accurate.

The remainder of the paper is organized as follows. In Section II, we present the lookup table idea to find RSMTs for low-degree nets. In Section III, we describe the algorithm to generate the POWVs and the POSTs. In Section IV, we show how the lookup table size can be reduced. In Section V, we derive a very efficient technique to evaluate all the POWVs for a given net. In Section VI, we present the net breaking technique for high-degree nets. In Section VII, we show the experimental results. The paper is concluded in Section VIII.

II. LOOKUP TABLE APPROACH FOR LOW-DEGREE NETS

We define a *net* of degree n to be a set of n pins. In this paper, we only consider Steiner trees along the Hanan grid as Hanan [16] pointed out that an optimal RSMT can always be constructed based on the Hanan grid. Given a net, the Hanan grid is formed by drawing one horizontal line and one vertical line through each pin. Let x_i be the x-coordinate of i -th vertical Hanan grid line such that $x_1 \leq x_2 \leq \dots \leq x_n$. Similarly, let y_j be the y-coordinate of j -th horizontal Hanan grid line such that $y_1 \leq y_2 \leq \dots \leq y_n$. Assume the pins are indexed in ascending order of y-coordinate. Let s_i be the rank of pin i if all pins are sorted in ascending order of x-coordinate. (Ties are broken arbitrarily for both x-coordinate and y-coordinate.) Therefore, the coordinates of pin i is (x_{s_i}, y_i) . The notations are illustrated in Figure 1. $s_1 s_2 \dots s_n$ is called the *position sequence* of the net. For the net in Figure 1, its position sequence is 3142. The position sequence completely specifies the relative positions of the pins.

Note that the length of a horizontal (respectively, vertical) edge in the Hanan grid is equal to the distance between two adjacent vertical (respectively, horizontal) Hanan grid lines. We denote *horizontal edge length* as $h_i = x_{i+1} - x_i$ and

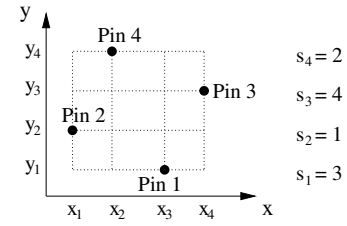


Fig. 1. Illustration of some notations.

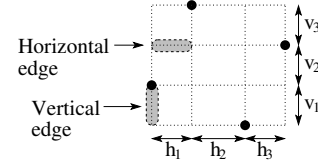


Fig. 2. An illustration of horizontal and vertical edge lengths.

vertical edge length as $v_i = y_{i+1} - y_i$ for $1 \leq i \leq n - 1$. These definitions are illustrated in Figure 2.

A Steiner tree on the Hanan grid can be decomposed into a collection of Hanan grid edges. So the wirelength of any Steiner tree can always be written as a linear combination of edge lengths such that all coefficients are positive integers. For example, for the net in Figure 1, the wirelength of the three possible Steiner trees shown in Figure 3(a), (b), and (c) can be written as $h_1 + 2h_2 + h_3 + v_1 + v_2 + 2v_3$, $h_1 + h_2 + h_3 + v_1 + 2v_2 + 3v_3$, and $h_1 + 2h_2 + h_3 + v_1 + v_2 + v_3$, respectively. For simplicity, we will express a wirelength as a vector of the coefficients, and call it a *wirelength vector*. For the Steiner trees in Figure 3(a), (b), and (c), the wirelength vectors are $(1, 2, 1, 1, 1, 2)$, $(1, 1, 1, 1, 2, 3)$, and $(1, 2, 1, 1, 1, 1)$, respectively.

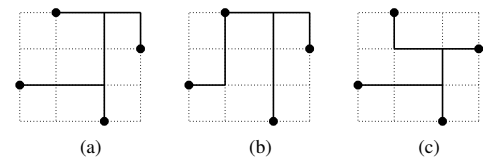


Fig. 3. Three possible Steiner trees for the net in Figure 1.

In order to find the optimal wirelength for a given net, we can enumerate all possible wirelength vectors. Note that although the number of possible Steiner trees is huge, the number of possible wirelength vectors is much less. More importantly, we notice that not all wirelength vectors have the potential to produce the optimal wirelength. Most vectors are redundant because they have a larger or equal value than another vector in all coefficients. For example, we can ignore the wirelength vector $(1, 2, 1, 1, 1, 2)$ because the wirelength produced by the vector $(1, 2, 1, 1, 1, 1)$ is always v_3 less. We called a vector that can potentially produce the optimal wirelength (i.e., cannot be ignored) a *potentially optimal wirelength vector* (POWV). We observe that for every low-degree net, there are only a few POWVs. For example, for all degree-3 nets, the only optimal wirelength vector is $(1, 1, 1, 1)$, which corresponds to the HPWL. For the net in Figure 1, the only two POWVs are $(1, 2, 1, 1, 1, 1)$ and $(1, 1, 1, 1, 2, 1)$.

Which one is optimal depends on which of h_2 and v_2 is smaller. All possible Steiner trees corresponding to these two wirelength vectors are given in Figure 4. Each of these trees is called a *potentially optimal Steiner tree* (POST). Some statistics on the number of POWVs will be given later in Table I.

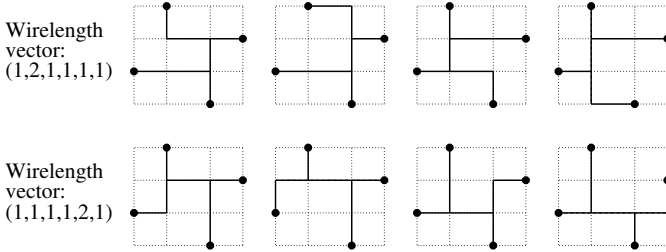


Fig. 4. All potentially optimal Steiner trees for the net in Figure 1.

If all the POWVs and the corresponding POSTs are pre-computed and stored in a lookup table, the RSMT will be easy to find. However, the number of different nets is infinite as the pin coordinates can take infinite different values. To handle this problem, we try to group together nets which can share the same set of POWVs. To see which nets can be grouped together, we first introduce the following definition. Two Steiner trees for two different nets are said to be *topologically equivalent* if they can be transformed to each other by changing the edge lengths (or equivalently, the distance between adjacent Hanan grid lines), with the restriction that their values remain positive. This concept is illustrated in Figure 5.

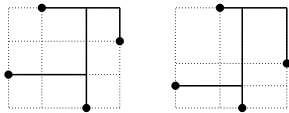


Fig. 5. Topologically equivalent Steiner trees for two different nets.

Lemma 1: If two nets have the same position sequence, then every Steiner tree of one net is topologically equivalent to a Steiner tree of the other net.

Proof: Suppose we shift the grid lines of the two Hanan grids for two nets so that they become identical. Since they have the same position sequence, the pins of the two nets are in the same locations in the Hanan grid. So every Steiner tree of one net will also be a Steiner tree of the other. ■

Theorem 1: The set of all degree- n nets can be divided into $n!$ groups according to the position sequence such that all nets in each group share the same set of POWVs.

Proof: Observe that the wirelengths of topologically equivalent Steiner trees can be expressed by the same wirelength vector. For example, the wirelength of the two trees in Figure 5 can both be represented by $(1, 2, 1, 1, 1, 2)$, although the values of h_i 's and v_i 's are different for the two nets. Based on this observation and Lemma 1, nets with the same position sequence can be grouped together to share the set of POWVs. Since the position sequence of a degree- n net is a permutation of $1, 2, \dots, n$, there should be $n!$ groups. ■

Our RSMT approach pre-computes the set of POWVs associated with each group and one² POST associated with each POWV. The POWVs and POSTs are stored in a lookup table. To compute the RSMT for a given net, we find out the position sequence of the net and then obtain the vectors for the corresponding group from the table. Each vector generates a wirelength by summing up the product of the vector entries with h_i 's and v_i 's. The minimum value over all vectors gives the optimal wirelength. The POST corresponding to the vector with minimum wirelength gives the RSMT.

III. GENERATION OF LOOKUP TABLE

In this section, we discuss the generation of the sets of POWVs and the associated POSTs. For each small net degree and for each group (i.e., position sequence), we may generate all possible Steiner trees on the Hanan grid, find the corresponding wirelength vectors, and prune away the redundant ones. The set of remaining vectors and trees are the POWVs and POSTs for the group. A trivial approach to generate all possible Steiner trees is to enumerate all possible combinations of using and not using each edge in the Hanan grid and check if the resulting sub-graph is a Steiner tree covering all the pins. However, this approach is extremely expensive. Even for degree 5, we need to enumerate a Hanan grid consisting of 40 edges for each of the 120 groups.

We propose a much more efficient algorithm based on a *boundary compaction* technique. For a given group, the boundary compaction technique reduces the grid size by compacting one of the four boundaries, i.e., shifting all pins on a boundary to the grid line adjacent to that boundary. The set of Steiner trees of the original problem can be generated by expanding the Steiner trees of the reduced grid back to the original grid. Figure 6 uses the compaction of left boundary as an example to illustrate the idea. Note that in Section II, we assume each Hanan grid line is associated with only 1 pin so that the concept of position sequence is well-defined. This assumption is not necessary unless we consider the grouping problem of a net. In this section, we assume a grid line may contain more than 1 pins so that grid lines can be combined and grid size can be reduced by boundary compaction.

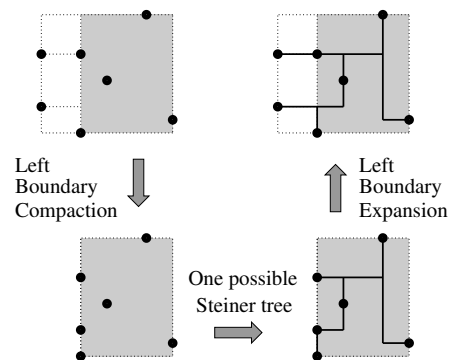


Fig. 6. An illustration of left boundary compaction.

²In general, more than one POSTs can be stored. Then different RSMTs of the same wirelength can be constructed. Routers may explore the alternatives to optimize some other objectives like congestion or timing.

We can route a net by performing boundary compaction and expansion recursively. By compacting the four boundaries in different order, a set of different Steiner trees with different wirelength vectors can be generated. Since we are performing the routing in a restricted way, it is possible that some Steiner trees and hence some wirelength vectors will not be generated. We define a grid G to be *compactable* if for each POWV V of G , there exists a boundary b such that V can be generated by expanding some POWV of the reduced grid obtained by compacting G at b . In other words, we can always reduce the size of a compactable grid without worrying about missing some POWVs. Lemmas 2, 3, and 4 below give several situations that a grid is compactable. The proofs of the lemmas are in Appendix I. An example of non-compactable grid is given in Figure 7(a). Figure 7(b) shows the optimal Steiner tree, which cannot be generated by boundary compaction.

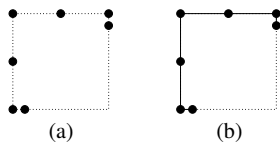


Fig. 7. An example of non-compactable grid.

Lemma 2: A grid G is compactable if it has a boundary with only one pin.

Lemma 3: A grid G is compactable if it has a corner with one pin P and both boundaries adjacent to P have exactly one other pin.

Lemma 4: A grid G is compactable if it has up to 6 pins at the four boundaries.

The algorithm to generate one POST for each POWV in a given group is presented in Figure 8. With the POSTs, the corresponding POWVs can be easily computed. Instead of enumerating all Steiner trees first and pruning the redundant ones (i.e., those not correspond to POWVs) at the end, we prune the redundant trees for each sub-problem. By performing pruning as early as possible, the efficiency of the algorithm can be significantly improved.

In Steps 1–2, we directly generate the POSTs when G consists of a single (horizontal or vertical) grid line or is a 2×2 grid. Steps 3–4 are based on Lemma 2, and Steps 5–8 are based on Lemma 3. Note that the proofs of these lemmas actually identify which boundaries to compact without missing any POWV. Since one or two (instead of four) recursive calls are made and these cases occur frequently for low-degree nets, the runtime of the algorithm can be dramatically reduced. If Lemmas 2 and 3 cannot be applied, we try compacting all four boundaries in Steps 14–17. Lemma 4 guarantees that for nets with up to 6 pins, all POWVs will be generated.

For grids with 7 or more pins, some POWVs may be missed by boundary compaction. So some extra Steiner trees are included in Steps 10–13. In Step 11, there are 7 trees in S . Each tree is a near-ring structure, which is the bounding box that surrounds the grid with edges connecting one of the 7 pairs of adjacent pins removed. Lemma 5 below proves that boundary compaction together with the near-ring structures are sufficient to generate all POWVs for degree-7 nets. The proof of Lemma 5 is in Appendix I.

Algorithm Gen-LUT(G)

Input: A grid G with some pins at grid nodes

Output: One POST for each POWV of the group associated with G

begin

1. If G is simple enough,
2. generate and return the set of POSTs for G
3. else if any boundary b contains only one pin,
4. return Expand- b (Gen-LUT(Compact- b (G)))
5. else if there is a corner with one pin such that
6. both its adjacent boundaries b_1 and b_2 have one other pin,
7. return Prune(Expand- b_1 (Gen-LUT(Compact- b_1 (G)))
8. \cup Expand- b_2 (Gen-LUT(Compact- b_2 (G)))
9. else
10. if there are 7 pins with all 7 pins on boundaries,
11. $S = \{\text{Trees with near-ring structure connecting all pins}\}$
12. else if there are ≥ 8 pins with ≥ 7 pins on boundaries,
13. $S = \text{Connect-adj-pins}(G, d)$ where $d = \# \text{ of pins} - 3$
14. return Prune($S \cup \text{Expand-left}(\text{Gen-LUT}(\text{Compact-left}(G)))$
15. $\cup \text{Expand-right}(\text{Gen-LUT}(\text{Compact-right}(G)))$
16. $\cup \text{Expand-top}(\text{Gen-LUT}(\text{Compact-top}(G)))$
17. $\cup \text{Expand-bot}(\text{Gen-LUT}(\text{Compact-bot}(G)))$

end

Fig. 8. The POST generation algorithm for a given group. For $b \in \{\text{left, right, top, bottom}\}$, Expand- b () and Compact- b () perform compaction and expansion of boundary b , respectively. Prune() performs pruning of redundant trees not corresponding to POWVs. Connect-adj-pins() is used to generate extra trees not producible by boundary compaction.

Lemma 5: For a grid with 7 pins, boundary compaction together with the near-ring structures can generate all POWVs.

For nets with 8 or more pins, we used a function Connect-adj-pins() to generate some extra trees. Connect-adj-pins(G, d) connects two or more adjacent pins on the same boundary by introducing a branch along the boundary. Those pins can be at a distance at most d grid lines away from each other. (See Figure 9(a) for an illustration.) Then those pins are replaced by a pseudo-pin located somewhere on the branch. For each possible location of the pseudo-pin, Gen-LUT() is recursively called to generate the POSTs of the reduced grid (as illustrated in Figure 9(b)). The POSTs of G can be constructed by combining the branch with the POSTs of all reduced grids. (See Figure 9(c).)

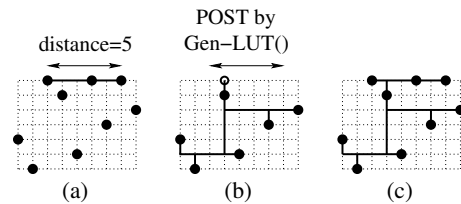


Fig. 9. An illustration for Connect-adj-pins(G, d) with $d \geq 5$.

Note that this technique is complementary to boundary compaction. It produces tree branches along a boundary that cannot be produced by boundary compaction. Lemma 6 below proves that boundary compaction together with Connect-adj-pins() are sufficient to generate all POWVs for nets with degree up to 10. The proof of Lemma 6 is in Appendix I.

Lemma 6: For a net with n pins where $7 \leq n \leq 10$, boundary compaction together with Connect-adj-pins() with distance $d = n - 3$ can generate all POWVs.

Note that Connect-adj-pins() can also be used to handle nets

Degree n	# of groups $n!$	# of POWVs in a group		
		Min.	Ave.	Max.
2	2	1	1	1
3	6	1	1	1
4	24	1	1.667	2
5	120	1	2.467	3
6	720	1	4.433	8
7	5040	1	7.932	15
8	40320	1	15.251	33
9	362880	1	30.039	79

TABLE I

NUMBER OF POWVs IN A GROUP FOR NETS OF A GIVEN DEGREE.

with 7 pins. However, Connect-adj-pins() is very slow because one recursive call to Gen-LUT() is made for each possible location of the pseudo-pin. Thus, the near-ring structure is used instead.

The completeness of the algorithm Gen-LUT() is summarized in the following theorem.

Theorem 2: The algorithm Gen-LUT() generates one POST for each POWV for nets with degree 10 or less.

Proof: This theorem follows directly from Lemma 4, Lemma 5 and Lemma 6. ■

The number of POWVs in a group is listed in Table I. We only generate the lookup table up to degree 9. The computation time for lookup table generation will be discussed at the end of Section IV as it is affected by the table size reduction techniques presented in Section IV.

IV. REDUCTION OF LOOKUP TABLE SIZE

According to Table I, for degree 9 alone, there are 10.9 million POWVs. If one byte is used to store each of the 16 entries in a POWV, the POWV storage requirement for degree 9 will be 166.3 MB. The POST associated with each POWV should have up to 7 Steiner nodes and $9+7-1 = 15$ branches. If one byte is used to store each branch in a POST, the POST storage requirement for degree 9 will be 155.9 MB. The total storage requirement for both POWVs and POSTs and for all degree up to 9 will be prohibitively large.

A smaller table will reduce the usage of hard disk, main memory and cache. It will also reduce the time of loading the lookup table from hard disk to memory. So it is desirable to reduce the size of the lookup table.

One technique to reduce the POWV storage requirement is to explore the similarity among POWVs in a group and store the differences between the POWVs according to the MST computed in Section V below. For this method, instead of using $2 \times (d-1)$ bytes for each POWV of degree d , we only need 2.5 bytes or less as shown in Table III. However, this method does not reduce the number of POWVs or the POST storage requirement.

Another technique is to explore the equivalence of different groups and show that the POWVs and POSTs of only a small fraction of all groups need to be generated and stored. Note that the table generation time will also be reduced by this technique.

Groups are equivalent for two reasons. First, observe that even though the nets in Figures 10(a) and 10(b) belong to two

different groups, both will become the grid in Figure 10(c) if the top boundary is compacted. Note that by Lemma 2, both grids are compactable at the top boundary. Hence, the two groups for these nets have the same set of POWVs. Moreover, even the POSTs can be shared between the groups. For example, POSTs corresponding to the POWV (1,2,1,1,1,1) for the nets in Figures 10(a) and 10(b) are shown in Figures 10(d) and 10(e), respectively. It is clear that both POSTs have the same topology (consisting of branches AE, BE, EC and CD). The same argument can be applied to all 4 boundaries. Therefore, up to $2^4 = 16$ different groups can share a set of POWVs and POSTs. (The number of equivalent groups may be less than 16 because pins can be shared by adjacent boundaries and so not all combinations exist.) Second, if two nets are symmetrical horizontally, vertically or diagonally, the POWVs and POSTs of one group can be transformed to those of the other. Due to the overhead in solution transformation, only horizontal symmetry is considered in our implementation. This allows two groups to share the POWVs and POSTs.

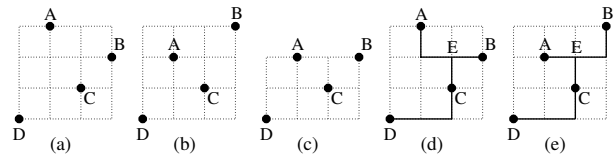


Fig. 10. Equivalence of different groups due to boundary compaction.

Some implementation details are described below. For any group of degree n such that the corresponding position sequence is $s_1 s_2 \dots s_n$, we define a modified position sequence $p_1 p_2 \dots p_n$ as follows:

$$p_i = |\{s_j : 1 \leq j < i \text{ and } s_j < s_i\}| \text{ for } 1 \leq i \leq n$$

For the example in Figure 1, $p_1 p_2 p_3 p_4 = 0021$. According to the definition above, it is not hard to see that p_i can take any integral value between 0 and $i-1$. We define a group index for the group as:

$$k = \prod_{j=1}^n \frac{n!}{j!} \times p_j$$

We prove in Lemma 7 below that group index can be used as the array index for the lookup table organized as an array of $n!$ groups. Then we prove in Lemma 8 that it is sufficient for the lookup table to be an array for only the first $n!/4$ groups. The proofs of both lemmas are in Appendix II.

Lemma 7: Group index is an one-to-one mapping from the groups of degree n to an integral value between 0 and $n!-1$.

Lemma 8: Any group of degree n is equivalent to a group with group index between 0 and $n!/4-1$.

Some statistics of the lookup table are listed in Table II. We generate the lookup table up to degree 9. By exploring the equivalence of groups, we can reduce the number of groups generated and stored by a factor of 25.8. (The table generation time should also be reduced by a similar factor.) The total table size is only 9.00 MB, which can be easily handled by today's computers.

Degree n	# of groups			Table size (MB)		Gen. time
	$n!$	generated	$n!$ /gen.	POWV	POST	
2	2	1	2	0.00	0.00	0.0 s
3	6	1	6	0.00	0.00	0.0 s
4	24	2	12	0.00	0.00	0.0 s
5	120	8	15	0.00	0.00	0.0 s
6	720	36	20	0.00	0.00	0.0 s
7	5040	222	22.70	0.01	0.02	0.0 s
8	40320	1638	24.62	0.17	0.31	50.7 s
9	362880	13950	26.01	2.56	5.93	58.2 hr
Total	409112	15858	25.80	2.75	6.26	58.2 hr

TABLE II
SOME STATISTICS OF THE LOOKUP TABLE.

The last column of Table II is the lookup table generation time in a PC with a 3.4 GHz Pentium 4 processor. It is extremely fast to generate the table up to degree 7 because of the boundary compaction technique and the near-ring structure presented in Section III. For degrees 8 and 9, the generation time is much longer because of the function Connect-adj-pins(). Note that we have several ideas to significantly reduce the table generation time (e.g., storing the solutions of a grid instead of recomputing them so that they can be reused in different recursive calls). However, as the lookup table only needs to be generated once, we did not implement those ideas.

V. SPEEDUP OF MINIMUM WIRELENGTH COMPUTATION

To find the optimal RSMT of a given net, we need to consider the set of POWVs in the corresponding group. A straightforward approach is to evaluate the POWVs independently. For each POWV $(\alpha_1, \alpha_2, \dots, \alpha_{n-1}, \beta_1, \beta_2, \dots, \beta_{n-1})$, we compute the expression $WL = \sum_{i=1}^{n-1} \alpha_i h_i + \sum_{i=1}^{n-1} \beta_i v_i$. Since entries in POWVs are typically small integers, and addition is computationally much less expensive than multiplication, it is more efficient to add the edge length several times instead of using multiplication. In addition, each of the edge length should be used at least once. So it is better to evaluate the expression as $WL = HPWL + \sum_{i=1}^{n-1} (\alpha_i - 1)h_i + \sum_{i=1}^{n-1} (\beta_i - 1)v_i$. Then we have $2(n-1)$ less terms to add.

However, we observe that most POWVs shared by a group of nets are very similar to one another. Many of them differ from other in only one or two entries. Hence, some POWVs can be efficiently evaluated by adding or subtracting some terms from some other previously computed POWVs. By exploring the dependency among the POWVs, the evaluation of all POWVs for a net can be made more efficient than the independent approach.

The problem of determining the best dependency among POWVs for a given group can be transformed into a minimum spanning tree problem. Consider a group associated with a set of q POWVs. We construct a complete graph with $q+1$ nodes. q of these nodes correspond to the q POWVs in the set and one more node corresponds to the wirelength vector $(1, \dots, 1, 1, \dots, 1)$ (i.e., HPWL). The weight of each edge is set to the 1-norm of the difference of the two corresponding wirelength vectors. In other words, the edge weight is equal to the number of addition/subtraction required to convert from

Degree n	Average # of ADD/SUB			
	per group		per POWV	
	Independent	MST	Independent	MST
2	0	0	0	0
3	0	0	0	0
4	1.333	1.333	0.8	0.8
5	4.267	4.267	1.73	1.73
6	14.422	10.333	3.253	2.331
7	39.651	20.025	4.999	2.525
8	109.136	38.561	7.156	2.528
9	288.060	74.155	9.590	2.469

TABLE III
AVERAGE NUMBER OF ADDITION/SUBTRACTION REQUIRED.

the wirelength of one vector to that of the other. Given a minimum spanning tree of the graph, we can evaluate the POWVs in an order defined by a breath-first traversal of the tree starting from the node corresponding to the HPWL. The total edge weight of the minimum spanning tree gives the number of addition/subtraction required to compute all q POWVs.

The average number of addition/subtraction required for the independent approach and the MST-based approach are listed in Table III. Columns two and three give the average number per group, which is proportional to the average runtime to evaluate a net. It is clear that the MST-based approach can significantly speed up the evaluation of high-degree nets. The last two columns give the average number per POWV, which is proportional to the average runtime to compute a POWV. It shows that for the independent approach, a lot more entries need to be added for POWVs of high-degree nets, while for the MST-based approach, the number of entries to be add/subtract first increases slowly with net degree and then remains around 2.5.

VI. NET BREAKING FOR HIGH-DEGREE NETS

For high-degree nets, both the table size and the number of operations to evaluate a net will be impractically large. So the table lookup approach is practical only for low-degree nets.

In FLUTE, we have a user-defined parameter D . A lookup table is constructed up to degree D ($D = 9$ in current implementation). Nets with degree higher than D are broken into several sub-nets with degree ranging from 2 to D to which the table lookup estimation can be applied.

In this section, we present a technique to recursively break high-degree nets. In this technique, if a net satisfies certain conditions, it will be broken optimally. Otherwise, four heuristics are applied to collectively determine a score for each way of breaking. Then several ways corresponding to the highest scores are tried by making recursive calls. In this technique, a scheme is also introduced to allow users to control the tradeoff between accuracy and runtime.

A. Optimal Net Breaking Algorithm

Theorem 3: For any net, if the set of pins can be partitioned into two sub-sets $L = \{\text{Pin } 1, \dots, \text{Pin } r\}$ and $R = \{\text{Pin } r + 1, \dots, \text{Pin } n\}$ such that the x-coordinate of any pin in L is

less than or equal to that of any pin in R (see Figure 11(a) for an example with $r = 3$), then an optimal RSMT can be constructed by merging the optimal RSMTs of $L \cup \{(x_r, y_r)\}$ and $\{(x_r, y_r)\} \cup R$.

Proof: In any optimal RSMT, there should be at least one³ “bridge” connecting the two sub-sets (Figure 11(b)). An optimal RSMT T^* that passes through the node (x_r, y_r) can be constructed by shifting the segments of each bridge without changing the wirelength (Figure 11(c)). Another RSMT T with the same or less wirelength to T^* can be obtained by merging the optimal RSMTs for the two sub-sets with the node (x_r, y_r) added to both. Hence, T should also be optimal. ■

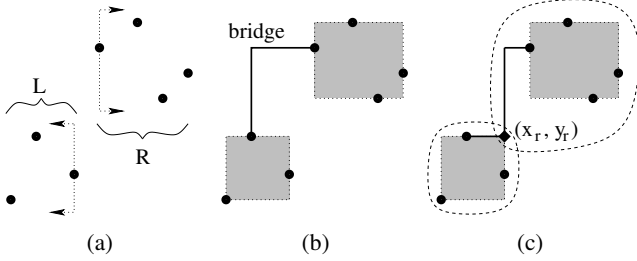


Fig. 11. Illustration of the optimal net breaking algorithm.

Theorem 4: For any net, if there exists r such that $s_i \geq n - r + 1$ for all $i \in \{1, \dots, r\}$, then an optimal RSMT can be constructed by merging the optimal RSMTs of $\{\text{Pin } 1, \dots, \text{Pin } r, (x_{n-r+1}, y_r)\}$ and $\{(x_{n-r+1}, y_r), \text{Pin } r + 1, \dots, \text{Pin } n\}$.

Proof: Similar to Theorem 3. ■

The optimal net breaking algorithm will break a net according to Theorems 3 and 4 if there exists $r \in \{2, \dots, n - 2\}$ satisfying either one of the two conditions. Note the size of the two sub-nets are $r + 1$ and $n - r + 1$. So it will not be useful to break the net if $r = 1$ or $n - 1$.

B. Net Breaking Heuristics

Without loss of generality, consider breaking the net according to y-coordinate. If the net is broken at pin r , then pin 1 to pin r will form one sub-net, and pin r to pin n will form another sub-net. To ensure that both sub-nets are at least a constant factor smaller than the original net, we require $\delta n \leq r \leq n - \delta n + 1$ for some positive constant δ . We compute a score which is a weighted sum of four components:

$$\text{Score } S(r) = S_1(r) - \alpha S_2(r) - \beta S_3(r) - \gamma S_4(r).$$

A larger score means a more desirable way of breaking. So it is better for $S_1(r)$ to be large, and for $S_2(r)$, $S_3(r)$ and $S_4(r)$ to be small.

The first component is:

$$S_1(r) = y_{r+1} - y_{r-1}$$

If we break the net at pin r , pin r will become the only pin at the bottom (respectively, top) boundary of the upper (respectively, lower) sub-net. According to Lemma 2, the edge

length $y_{r+1} - y_r$ (respectively, $y_r - y_{r-1}$) will be counted once in the wirelength of the upper (respectively, lower) sub-net. Otherwise, both $y_{r+1} - y_r$ and $y_r - y_{r-1}$ are likely to be counted more than once in the total wirelength. So it is better to break the net at pin r if $y_{r+1} - y_{r-1}$ is large.

The second component is:

$$S_2(r) = \begin{cases} 2(x_3 - x_2) & \text{if } s_r = 1 \text{ or } 2 \\ x_{s_r+1} - x_{s_r-1} & \text{if } 3 \leq s_r \leq n - 2 \\ 2(x_{n-1} - x_{n-2}) & \text{if } s_r = n - 1 \text{ or } n \end{cases}$$

When $3 \leq s_r \leq n - 2$, x_{s_r+1} and x_{s_r-1} are the x-coordinates of the pins just right and just left of pin r , respectively. If we break the net at pin r , in both the lower sub-net and the upper sub-net, the pins on the left of pin r needs to be connected to those on the right (unless for the rare cases that there is no pin either on the left or on the right of pin r in a sub-net). So the edge lengths $x_{s_r+1} - x_{s_r}$ and $x_{s_r} - x_{s_r-1}$ will be counted in both the upper and the lower sub-nets. Therefore, it is less desirable to break the net at a pin with a large $x_{s_r+1} - x_{s_r-1}$. When $s_r = 1$ (respectively, n), pin r is at the left (respectively, right) boundary and x_{s_r-1} (respectively, x_{s_r+1}) is not defined. When $s_r = 2$ (respectively, $n - 1$), as the edge length $x_2 - x_1$ (respectively, $x_n - x_{n-1}$) will always be counted once for any way of breaking according to Lemma 2, it is less effective to use $x_{s_r+1} - x_{s_r-1}$ as a prediction. For these cases, we observe that it is good in practice to set the second component to either $2(x_3 - x_2)$ or $2(x_{n-1} - x_{n-2})$.

The third component is:

$$S_3(r) = \left| s_r - \frac{n+1}{2} \right| \times \bar{h} + \left| r - \frac{n+1}{2} \right| \times \bar{v}$$

where $\bar{h} = \frac{x_{n-1} - x_2}{n - 3}$ and $\bar{v} = \frac{y_{n-1} - y_2}{n - 3}$. In general, it is better to have the breaking pin closer to the center of the net. If pin r is close to center vertically (i.e., r is close to $(n+1)/2$), the net will be evenly divided and hence less recursive calls are likely to be made later. Both accuracy and runtime will be improved as a result. If pin r is close to center horizontally (i.e., s_r is close to $(n+1)/2$), other pins are closer to pin r on average in both upper and lower sub-nets. In here, we use the distance of pin r from the center (in terms of number of edges in Hanan grid) to predict how many extra edges need to be used. \bar{h} and \bar{v} are the average edge lengths in the Hanan grid. Because $x_n - x_{n-1}$, $x_2 - x_1$, $y_n - y_{n-1}$, and $y_2 - y_1$ are always counted once for any solutions, they are not included in the computation of average length of extra edges. In principle, we can use different weights for the horizontal part and the vertical part of S_3 to form the score. However, we observe that a single weight β works just as well.

The fourth component $S_4(r)$ is the total half-perimeter wirelength (HPWL) of the two sub-nets. This is a direct way to predict the resulting wirelength.

We experimentally determined that it is good to set α to 0.3, β to $7.4/(n+10)$, and γ to $4.8/(n-1)$. S_1 is the most important of the four components. It produces significantly better results with the single term S_1 than with any one of the other three. The result is even better by combining all four.

After sub-trees for the two sub-nets are constructed, they are combined to form a Steiner tree for the original net. Note that

³It can be proved that there is always exactly one bridge.

the two sub-trees may share some edges as shown in Figure 12(a). These redundant edges can be detected in constant time and will be removed by introducing an extra Steiner node as shown in Figure 12(b). To further reduce wirelength, a local refinement technique can be applied to improve the subtree in the neighborhood of the breaking pin. This technique uses FLUTE to reconstruct the subtree connecting all pins that are directly reachable from the breaking pin without passing through other pins (as illustrated in Figure 12(c)). To minimize the runtime overhead, the local refinement technique is applied only if the subtree around the breaking pin has up to D pins.

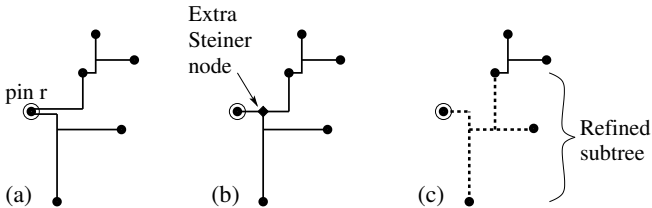


Fig. 12. Merging two Steiner sub-trees.

C. Accuracy Control Scheme

We can control the accuracy of FLUTE by changing the number of ways of breaking each net. However, we observe that it is not as good if all sub-nets generated by recursive calls are handled with the same accuracy. A better tradeoff between accuracy and runtime can be obtained if lower-level sub-nets are handled with less accuracy. We introduce a user-defined accuracy parameter A . The original net is handled with accuracy A . That means A different ways of breaking are tried. Then for each recursive call, the accuracy is set to $\max\{\lfloor A/2 \rfloor, 1\}$. We notice that a small A is already enough to obtain very accurate solutions. We set the default value of A to 3.

D. Time Complexity of FLUTE

The time complexity is analyzed as follows. Consider $A = 1$. We first need to sort all pins according to x - and y -coordinates. Then we recursively break the net into two sub-nets in a roughly even manner. In each recursive call, it takes linear time to check the optimal breaking conditions and to compute the scores. So the total runtime is $O(n \log n)$. Note that the optimal net breaking algorithm may not break the net in an even manner. However, we can implement the algorithm to search for clusters simultaneously starting from all four corners (instead of only lower-left and lower-right corners as suggested by Theorem 3 and 4, respectively). Then, if the net is not broken evenly (i.e., a small cluster exists), the checking time will also be small. So the total runtime will still be $O(n \log n)$. For accuracy A , it is not hard to show by mathematical induction on A that the time complexity of FLUTE is $O(A^{\frac{\log A + 1}{2}} n \log n)$.

Circuit	# of nets	Ave. degree	Max. degree
ibm01	14111	3.58	42
ibm02	19584	4.15	134
ibm03	27401	3.41	55
ibm04	31970	3.31	46
ibm05	28446	4.44	17
ibm06	34826	3.68	35
ibm07	48117	3.65	25
ibm08	50513	4.06	75
ibm09	60902	3.65	39
ibm10	75196	3.96	41
ibm11	81454	3.45	24
ibm12	77240	4.11	28
ibm13	99666	3.58	24
ibm14	152772	3.58	33
ibm15	186608	3.84	36
ibm16	190048	4.10	40
ibm17	189581	4.54	36
ibm18	201920	4.06	66
All	1570355	3.92	134

TABLE IV
BENCHMARK INFORMATION.

VII. EXPERIMENTAL RESULTS

The FLUTE algorithm described in this paper is implemented in C in the software package FLUTE-2.5. For our implementation, the runtime complexity is $O(n^2)$ because a simple $O(n^2)$ sorting algorithm is used, and the net breaking pin is searched in the range $3 \leq r \leq n - 2$. To minimize runtime, the local refinement technique introduced in Section VI-B is not applied for low accuracy (i.e., when $A \leq 4$). The source code of FLUTE is posted in the ‘‘Rectilinear Spanning and Steiner Trees’’ slot of the GSRC bookshelf [17].

We perform all experiments in a 3.4-GHz Intel Pentium 4 machine⁴. Three sets of experiments are conducted. First, we compare the following six algorithms on nets from industrial circuits: an efficient $O(n^2)$ implementation of Prim’s algorithm (RMST) [15], Refined Single Trunk Tree (RST-T) [13], the spanning graph based RSMT algorithm (SPAN) [9], the batched greedy triple contraction algorithm (BGA) [11], the near-optimal Batched Iterated 1-Steiner (BIIS) heuristic [6], and FLUTE with default accuracy $A = 3$. The exact RSMT software GeoSteiner 3.1 [5] is used to generate the optimal solutions. Source codes of RMST, BGA, BIIS, and GeoSteiner are downloaded from the GSRC Bookshelf [20]. Source codes of SPAN and RST-T are obtained from the authors. The 18 IBM circuits in the ISPD98 benchmark suite are used. Some information of the benchmark circuits are given in Table IV. There are totally 1.57 million nets. The placement is generated by FastPlace [21].

The wirelength comparison is shown in Table V. FLUTE is the best among the six algorithms. The average wirelength error over all nets is only 0.075%. FLUTE produces the best wirelength for all 15 circuits in which all nets have degree 55 or less. BIIS is the best for the remaining three circuits (ibm02, ibm08 and ibm18).

The breakdown of the wirelength estimation for nets with different degree is shown in Table VI. A summary of all 18

⁴In earlier versions of this paper [18], [19], experiments are performed in a Sun Sparc-2 machine. For unknown reasons, BIIS is significantly slower in Sun machines.

Degree	Net breakdown		Wirelength error (%)					
	#	WL	RMST	RST-T	SPAN	BGA	BIIS	FLUTE
2	54.92%	27.98%	0.00	0.00	0.00	0.00	0.00	0.00
3	14.40%	10.26%	2.50	0.00	0.03	0.00	0.00	0.00
4	7.68%	7.84%	3.89	0.00	0.11	0.00	0.00	0.00
5	5.61%	8.18%	4.74	0.00	0.21	0.07	0.05	0.00
6	3.20%	5.65%	5.40	0.49	0.29	0.12	0.07	0.00
7	2.28%	4.82%	5.91	1.02	0.37	0.13	0.09	0.00
8	1.98%	4.61%	6.25	1.91	0.42	0.16	0.12	0.00
9	1.81%	4.46%	6.79	2.65	0.48	0.21	0.15	0.00
10–17	6.98%	21.72%	7.81	6.21	0.60	0.29	0.22	0.16
≥18	1.15%	4.48%	9.04	14.05	0.75	0.40	0.32	0.87

TABLE VI

BREAKDOWN OF THE WIRELENGTH ESTIMATION ACCORDING TO DEGREE FOR NETS OF ALL 18 CIRCUITS.

Circuit	Wirelength error (%)					
	RMST	RST-T	SPAN	BGA	BIIS	FLUTE
ibm01	4.092	1.933	0.251	0.129	0.106	0.074
ibm02	5.849	3.780	0.331	0.143	0.115	0.209
ibm03	4.637	1.919	0.271	0.125	0.095	0.062
ibm04	4.048	1.255	0.203	0.084	0.060	0.051
ibm05	4.489	3.134	0.329	0.153	0.112	0.106
ibm06	5.964	2.822	0.381	0.182	0.134	0.084
ibm07	4.720	1.704	0.268	0.116	0.084	0.046
ibm08	4.784	4.445	0.328	0.162	0.123	0.261
ibm09	4.331	1.804	0.235	0.105	0.075	0.042
ibm10	4.104	1.790	0.252	0.104	0.080	0.051
ibm11	4.018	1.227	0.219	0.087	0.062	0.024
ibm12	3.783	1.908	0.248	0.106	0.077	0.054
ibm13	4.782	2.002	0.292	0.135	0.102	0.053
ibm14	3.908	1.540	0.221	0.095	0.068	0.040
ibm15	4.201	1.941	0.266	0.106	0.077	0.062
ibm16	4.231	2.421	0.279	0.124	0.090	0.068
ibm17	3.905	2.188	0.263	0.110	0.082	0.056
ibm18	4.432	3.353	0.300	0.134	0.100	0.147
All	4.232	2.261	0.269	0.117	0.086	0.075

TABLE V

PERCENTAGE ERROR IN WIRELENGTH.

Circuit	Runtime (s)					
	RMST	RST-T	SPAN	BGA	BIIS	FLUTE
ibm01	0.02	0.09	0.55	0.75	1.01	0.02
ibm02	0.02	0.14	1.05	1.50	4.32	0.03
ibm03	0.02	0.18	1.02	1.38	1.95	0.03
ibm04	0.04	0.20	1.07	1.44	2.24	0.02
ibm05	0.03	0.20	1.71	2.40	2.69	0.05
ibm06	0.03	0.23	1.45	1.95	2.53	0.04
ibm07	0.05	0.32	1.96	2.59	3.26	0.04
ibm08	0.06	0.35	2.63	3.74	6.60	0.09
ibm09	0.07	0.40	2.42	3.19	4.13	0.06
ibm10	0.08	0.53	3.59	4.77	5.85	0.09
ibm11	0.06	0.53	2.87	3.76	5.16	0.05
ibm12	0.10	0.54	3.94	5.33	6.25	0.10
ibm13	0.10	0.66	3.89	5.18	6.68	0.09
ibm14	0.15	1.02	5.91	7.84	10.11	0.14
ibm15	0.21	1.27	8.18	10.86	13.96	0.22
ibm16	0.23	1.33	9.33	12.47	14.75	0.26
ibm17	0.28	1.39	11.06	15.06	16.63	0.31
ibm18	0.26	1.40	9.81	13.28	17.82	0.30
All	0.93	5.56	37.34	50.25	64.92	1.0

TABLE VII

RUNTIME COMPARISON. THE OVERALL RUNTIMES IN THE LAST ROW ARE NORMALIZED WITH RESPECT TO FLUTE RUNTIME.

circuits is given. Columns 2 and 3 provide a breakdown on the number of nets and the wirelength. Notice that although most nets are of degree two or three, there are still a substantial proportion of higher degree nets and the contribution of those nets to the wirelength is very significant. For example, nets with degree 10 or more account for 8.13% of all nets and contribute 26.2% of total wirelength. Columns 4 to 9 report the percentage error in wirelength. As the table shows, all six techniques have more error for nets with higher degree. FLUTE is exact for nets up to degree 9 and is still very accurate for higher degree nets. Note that although RST-T is exact up to degree 5, it performs badly for high-degree nets. As a result, the overall accuracy is far worse than the other four RSMT algorithms.

The runtime comparison is listed in Table VII. Note that FLUTE is much faster than all the other Steiner tree algorithms although it is the most accurate. FLUTE is only 7% slower than RMST.

Second, we show the effect of the accuracy parameter A to the tradeoff between wirelength error and runtime. A is varying from 1 to 12. A potential application of FLUTE is wirelength estimation. So an implementation of FLUTE with RSMT construction disabled and the widely-used HPWL are also compared. The average percentage error and total runtime

for all nets in 18 IBM circuits are reported in Table VIII.

Table VIII shows that the accuracy control scheme provides a very effective way to achieve much less error in a moderate runtime increase. The runtime is increasing at a rate much slower than $A^{\frac{\log A+1}{2}}$ because most nets have a low degree. We notice that if RSMT is not constructed, the runtime is decreased by roughly 1.3–2.1 \times . However, because the redundant edge removal and the local refinement techniques described at the end of Section VI-B cannot be used, the error is increased. For applications in which only wirelength estimation is required, such an implementation provides a much better tradeoff between accuracy and runtime unless extremely accurate solutions are desired. For extremely accurate solutions, the implementation with RSMT construction is more efficient even if the RSMT returned is not used.

Even with RSMT construction and a relatively high accuracy of $A = 3$, FLUTE is only 5.88 \times slower than HPWL while much more accurate. If RSMT is not required and an accuracy of $A = 1$ is sufficient, FLUTE is less than 3 \times slower than HPWL.

Third, we investigate the accuracy and runtime of different algorithms for nets with degree ranging from 10 to 100. We notice that out of 1.57 millions nets in 18 IBM circuits, only

Degree	Wirelength error (%)												
	RMST	RST-T	SPAN	BGA	BIIS	FLUTE							
						A = 1	A = 2	A = 3	A = 4	A = 6	A = 8	A = 10	A = 12
10	11.982	5.091	0.949	0.443	0.349	0.684	0.236	0.112	0.072	0.027	0.020	0.020	0.020
20	12.168	14.370	1.019	0.518	0.421	2.181	1.265	0.961	0.590	0.281	0.150	0.119	0.098
30	12.551	21.896	1.136	0.619	0.552	2.992	2.171	1.846	1.161	0.642	0.430	0.357	0.292
40	12.727	28.987	1.121	0.624	0.556	3.516	2.718	2.388	1.709	1.096	0.751	0.670	0.554
50	12.684	35.346	1.143	0.628	0.567	3.955	3.214	2.867	2.193	1.475	1.044	0.931	0.766
60	12.729	42.110	1.192	0.647	0.580	4.288	3.571	3.252	2.557	1.839	1.280	1.160	0.971
70	12.848	47.984	1.148	0.630	0.557	4.553	3.865	3.558	2.912	2.136	1.578	1.442	1.185
80	12.862	53.404	1.195	0.639	0.573	4.762	4.168	3.813	3.149	2.344	1.712	1.587	1.361
90	12.889	59.007	1.201	0.669	0.590	4.896	4.339	4.027	3.411	2.582	1.926	1.809	1.563
100	12.867	64.770	1.210	0.678	0.599	5.098	4.523	4.270	3.658	2.790	2.126	2.000	1.721

TABLE IX
PERCENTAGE ERROR IN WIRELENGTH FOR NETS OF DIFFERENT DEGREE.

Degree	Runtime (s)												
	RMST	RST-T	SPAN	BGA	BIIS	FLUTE							
						A = 1	A = 2	A = 3	A = 4	A = 6	A = 8	A = 10	A = 12
10	0.00	0.01	0.19	0.28	0.18	0.00	0.00	0.00	0.01	0.01	0.01	0.01	0.01
20	0.01	0.02	0.51	0.81	0.93	0.01	0.02	0.02	0.04	0.11	0.21	0.32	0.53
30	0.02	0.03	0.85	1.44	2.81	0.02	0.03	0.04	0.07	0.23	0.52	0.82	1.60
40	0.03	0.04	1.19	2.14	6.48	0.02	0.04	0.06	0.12	0.38	0.92	1.43	2.77
50	0.05	0.04	1.55	2.91	12.43	0.04	0.06	0.08	0.16	0.53	1.37	2.12	4.16
60	0.07	0.04	1.92	3.74	21.27	0.04	0.07	0.11	0.21	0.70	1.86	2.87	5.67
70	0.09	0.06	2.29	4.67	33.29	0.06	0.10	0.12	0.25	0.88	2.39	3.67	7.32
80	0.11	0.06	2.69	5.59	49.12	0.07	0.10	0.15	0.30	1.05	2.94	4.51	9.08
90	0.13	0.07	3.24	6.54	70.96	0.08	0.12	0.17	0.35	1.22	3.47	5.38	10.83
100	0.16	0.08	3.85	7.65	97.64	0.10	0.15	0.19	0.41	1.41	4.07	6.28	12.76

TABLE X
TOTAL RUNTIME FOR 1000 NETS OF DIFFERENT DEGREE.

1212 (0.077%) have a degree of more than 30, and only 80 (0.005%) have a degree of more than 60. So for VLSI applications, it should be enough to observe the behavior of algorithms for degree up to 100. 1000 nets are randomly generated for each degree. The average wirelength error and total runtime are reported in Table IX and Table X, respectively.

From Table IX and Table X, for nets with degree 10 to 30, FLUTE is clearly the best algorithm. It can be as fast as extremely fast algorithms (RMST and RST-T) yet much more accurate. It can also be more accurate than very accurate algorithms (SPAN, BGA and BIIS) yet much faster. (Note that the advantages of FLUTE over other algorithms in both accuracy and runtime are even more significant for nets with degree 9 or less as solutions can be obtained directly from the lookup table.)

For higher degree nets, FLUTE with a small A value can generate reasonably accurate solutions in a very short runtime. Other algorithms are either far less accurate or much slower. So FLUTE is still the most suitable algorithm for higher degree nets if moderate accuracy is enough. If very accurate solutions (say <2% error) are desired for nets with degree 50 or more, a large A value is required for FLUTE. In that case, FLUTE may not be the fastest algorithm.

VIII. CONCLUSION

In this paper, we introduced a fast and accurate lookup table based RSMT algorithm called FLUTE. The table stores for low-degree nets the set of POWVs associated with each position sequence and an RSMT topology associated with

each POWV. We proposed an algorithm based on boundary compaction to generate the sets of POWVs up to degree 9. We designed a MST-based approach to determine the most efficient way to evaluate each set of POWVs. We presented a net breaking technique to divide a high degree net into low-degree nets so that the table lookup estimation can be used. We also presented a scheme to allow users to control the tradeoff between accuracy and runtime. The experimental results with industrial nets showed that FLUTE with default accuracy is more accurate than the Batched 1-Steiner heuristic and is almost as fast as RMST construction.

APPENDIX I: PROOFS FOR SECTION III

This appendix contains the proofs of the lemmas regarding the optimality of the lookup table generation algorithm described in Section III. Lemmas 2–6 are directly used in Section III. However, in order to prove these lemmas, two additional lemmas (Lemmas 9 and 10) are required. They are added to the end of the appendix.

Lemma 2: A grid G is compactable if it has a boundary with only one pin.

Proof: Assume without loss of generality that the left boundary of G has only one pin P . Let G' be the reduced grid obtained by compacting G at the left boundary. So the first entry in the POWVs of G corresponds to the compacted edges. We show that every POWV V of G must be in the form $(1, V')$ where V' is a POWV of G' . Consider any POST T associated with V . We can prove that it has exactly one branch from P to other pins. If there are multiple branches from P

Algorithm	WL error (%)	Runtime		
		(s)	Normalized	
FLUTE (return RSMT)	$A = 1$	0.2313	1.27	0.65
	$A = 2$	0.1092	1.60	0.82
	$A = 3$	0.0747	1.94	1.00
	$A = 4$	0.0396	2.65	1.37
	$A = 5$	0.0243	3.88	2.00
	$A = 6$	0.0174	5.22	2.69
	$A = 7$	0.0154	5.93	3.06
	$A = 8$	0.0113	8.70	4.48
	$A = 9$	0.0104	9.63	4.96
	$A = 10$	0.0090	12.29	6.34
	$A = 11$	0.0086	13.39	6.90
	$A = 12$	0.0073	19.07	9.83
FLUTE (no RSMT)	$A = 1$	0.2721	0.98	0.51
	$A = 2$	0.1318	1.16	0.60
	$A = 3$	0.0917	1.37	0.71
	$A = 4$	0.0513	1.84	0.95
	$A = 5$	0.0430	2.08	1.07
	$A = 6$	0.0322	2.69	1.39
	$A = 7$	0.0292	3.02	1.56
	$A = 8$	0.0222	4.27	2.20
	$A = 9$	0.0209	4.76	2.45
	$A = 10$	0.0186	5.90	3.04
	$A = 11$	0.0178	6.42	3.31
	$A = 12$	0.0157	8.98	4.63
HPWL	-8.7710	0.33	0.17	

TABLE VIII

WIRELENGTH ERROR AND RUNTIME OF FLUTE FOR DIFFERENT ACCURACY A . THE ROW IN BOLD IS THE DEFAULT.

to other pins (as in Figure 13(a)), another Steiner tree with a single branch can be constructed as follows. Let l be the second Hanan grid line from the left boundary. The edges of T on the left of l can be replaced with a vertical segment along l connecting the subtrees of T on the right of l and a horizontal edge from P to the segment (as in Figure 13(b)). The POWV of this tree is better than V in the first entry and is at least as good in all other entries, contrary to the fact that V is potentially optimal. Hence, any POST must have a single branch from P , which implies the first entry of V should be 1. Moreover, if the branch does not go horizontally from P (as shown in Figure 13(c)), it can be “flipped” (as in Figure 13(d)) to obtain a tree with the same wirelength vector as V . By shifting P along the horizontal branch until the next Hanan grid line, the grid becomes G' . Hence the remaining entries of V should form a POWV of G' . ■

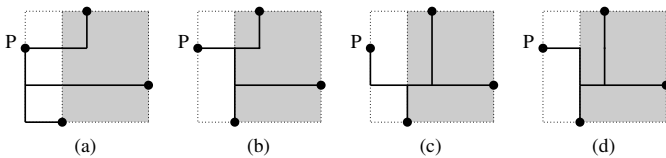


Fig. 13. Illustrations for the proof of Lemma 2.

Lemma 3: A grid G is compactable if it has a corner with one pin P and both boundaries adjacent to P have exactly one other pin.

Proof: Assume without loss of generality that P is at the lower left corner as illustrated in Figure 14(a). Assume on the contrary that there is a POWV of G such that its entries associated with all four boundaries are better than those obtained by boundary compaction. Consider any Steiner tree associated with this POWV. By Lemma 9, for both the left and

the bottom boundaries, the two pins should be connected by a branch along the boundary as illustrated in Figure 14(b). If G has no other pins besides the three, G is obviously compactable. Otherwise, these three pins should be connected to the rest of the tree by a branch. Suppose without loss of generality that the branch is originated from the left boundary as illustrated in Figure 14(c). Such a solution is not better than those obtained by compacting the left boundary. It contradicts to the assumption. Hence, G must be compactable. ■

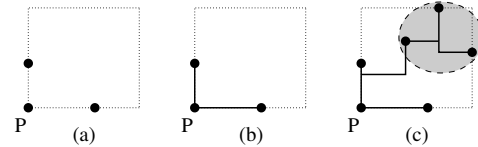


Fig. 14. Illustrations for the proof of Lemma 3.

Lemma 4: A grid G is compactable if it has up to 6 pins at the four boundaries.

Proof: If G has a boundary with only one pin, then Lemma 2 shows that it is compactable. So we focus on G with at least 2 pins on each boundary. As G has at most 6 pins on the boundaries and each boundary has at least 2 pins, at least two corners should have a pin so that it can be shared by two boundaries. All cases that satisfy the conditions above are shown in Figure 15. Note that only pins on the boundaries are considered. Also note that cases which are symmetrical to one of those in Figure 15 are not shown.

Lemma 3 can be applied to show that all cases except (f) are compactable. (The pin P can be the one at the lower left corner.) Lemma 10 can be applied to show that case (f) is also compactable. Therefore, a grid with 6 or less pins at the boundaries is always compactable. ■

Lemma 5: Boundary compaction together with the near-ring structures can generate all POWVs for a grid with 7 pins.

Proof: Consider a grid G with 7 pins that is not compactable. By Lemma 4, all 7 pins should be on the boundaries. By Lemma 2, there should be at least 2 pins on each boundary. As G has 7 pins at the boundaries and each boundary has at least 2 pins, at least one corner should have a pin so that it can be shared by two boundaries. All cases that satisfy the conditions above are shown in Figure 16. Note that cases which are symmetrical to one of those in Figure 16 are not shown.

Lemma 3 can be applied to show that cases (a), (b), (e), (h), (i), (j), (k), (m), (n) and (o) are compactable. Lemma 10 can be applied to show that cases (c), (g) and (l) are compactable.

It is not hard to see that cases (d) and (f) are not compactable. However, we can prove that the POWVs missed by boundary compaction are all covered by the near-ring structures. Assume it is not the case. In other words, there is a POWV missed by boundary compaction such that the associated Steiner tree has some branches not along the boundaries. We consider two cases:

- *Case 1) Those branches only connect adjacent boundaries.* Then those branches can be “flipped” such that all branches of the Steiner tree are along the boundaries.

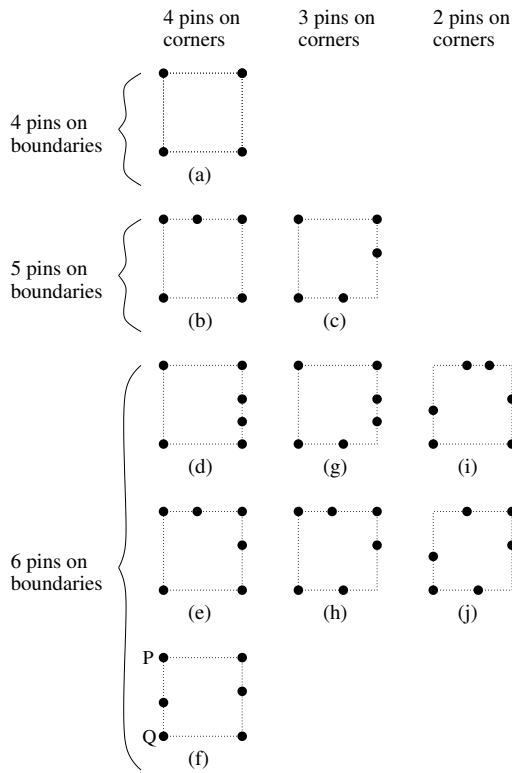


Fig. 15. Illustrations for the proof of Lemma 4.

Moreover, the resulting POWV is the same or better. Hence, the POWV can be generated by the near-ring structures.

- *Case 2) Those branches also connect two non-adjacent (i.e., opposite) boundaries.* Consider case (f). Assume without loss of generality that the left and right boundaries are connected by branches not along the boundaries. By Lemma 9, the two pins at the bottom boundary should be connected by a branch along the boundary. Also, at least two of the three pins at the top boundary should be connected by a branch along the boundary. If the left two pins are connected, such a solution is not better than those obtained by compacting the grid at the left boundary. If the right two pins are connected, such a solution is not better than those obtained by compacting the grid at the right boundary. Similar arguments can be applied to handle case (d). ■

Lemma 6: For a net with n pins where $7 \leq n \leq 10$, boundary compaction together with Connect-adj-pins() with distance $d = n - 3$ can generate all POWVs.

Proof: A net with n pins corresponds to a $n \times n$ Hanan grid such that each grid line has one pin. By Lemma 2, all 4 boundaries can be compacted once so that a $(n - 2) \times (n - 2)$ grid G is formed. Any two pins on the same boundary of G are at a distance at most $n - 3$ grid lines apart. Hence, Connect-adj-pins($G, n - 3$) can generate any branch along any boundary of G .

The only remaining issue is that boundary compaction may not be able to generate the branches originating from a branch

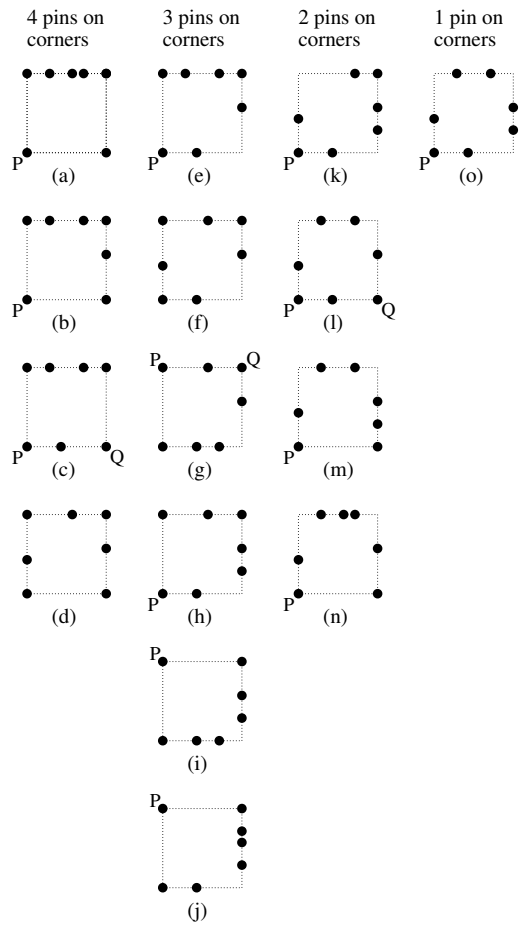


Fig. 16. Illustrations for the proof of Lemma 5.

introduced by Connect-adj-pins(). The reason is that after Connect-adj-pins() connects several pins on a boundary by a branch B , those pins are replaced by a single pseudo-pin. If there are more than one branches connecting B to the remaining pins in a POST, compacting that boundary will not generate this POST. (See Figure 17(a) for an illustration.)

We show in the following that if a net has 10 pins or less, there always exists a boundary such that boundary compaction can be applied. For any branch B introduced by Connect-adj-pins() in a boundary that cannot be compacted, the number of pins on B should be more than the number of branches connecting B to the remaining pins. Otherwise, this boundary can be compacted directly without even applying Connect-adj-pins(). So there should be at least 3 pins on B . As there are at most 10 pins in the grid, it is impossible to have at least 3 pins on each boundary unless some corner pins are shared. It is impossible to share all 4 corners because a ring (i.e., non-tree) structure will be formed. Consider the case that 3 corner pins are shared as shown in Figure 17(b). There should be at least 9 pins on boundaries. Besides, there should be at least two others pins (P and Q) not on boundaries. This case is impossible as the total number of pins is at least 11. It is not hard to see that if less than 3 corner pins are shared, even more pins are required to make the grid not compactable. ■

The following lemma is used in the proof of Lemma 3, Lemma 5 and Lemma 10.

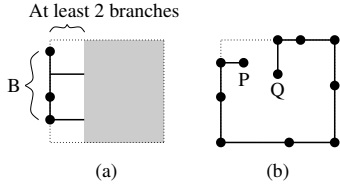


Fig. 17. Illustrations for the proof of Lemma 6.

Lemma 9: If a grid G is not compactable, then for any POST associated with any POWV missed by boundary compaction, there should be a branch connecting at least two pins along each of the four boundaries.

Proof: By Lemma 2, there should be at least two pins on each boundary. Without loss of generality, consider the pins on the left boundary. The lemma claims that at least two pins are connected by a branch along the left boundary as shown in Figure 18(a). Otherwise, each pin should be connected to the rest of the tree by a separate branch as shown in Figure 18(b). Such a solution is not better than those generated by compacting the left boundary. ■

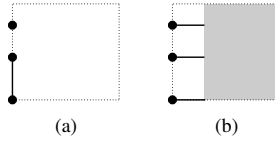


Fig. 18. Illustrations for the proof of Lemma 9.

The following lemma is used in the proof of Lemma 4 and Lemma 5.

Lemma 10: A grid G is compactable if it has two adjacent corners with pins P and Q , and each of the three boundaries involving P and Q has exactly one other pin.

Proof: Assume without loss of generality that P is at the lower left corner and Q is at the lower right corner as illustrated in Figure 19(a). Assume on the contrary that there is a POWV of G such that its entries associated with all four boundaries are better than those obtained by boundary compaction. Consider any Steiner tree associated with this POWV. By Lemma 9, for both the left and the right boundaries, the two pins should be connected by a branch along the boundary as illustrated in Figure 14(b). Moreover, pin Y should be connected to at least one of the corner pins P and Q by a branch along the bottom boundary. Without loss of generality, assume Y is connect to P as shown in Figure 19(b).

The subtree consisting of P , X and Y should be connected to the rest of the tree by a branch. If the branch is originated from the left boundary, such a solution is not better than those obtained by compacting the left boundary. If the branch is originated from the bottom boundary and it is not along the bottom boundary, such a solution is not better than those obtained by compacting the bottom boundary. If the branch is originated from the bottom boundary and it is along the bottom boundary (i.e., the branch connects Y and Q as shown in Figure 19(c)), we consider two cases based on whether there are other pins besides the five. If there is no other pin, G is obviously compactable from the top boundary. Otherwise, the

subtree consisting of the five pins should be connected to the other pins by a branch. If the branch is originated from the left/bottom/right boundary, such a solution is not better than those obtained by compacting the left/bottom/right boundary. ■

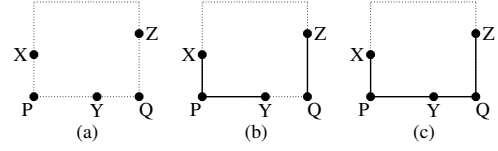


Fig. 19. Illustrations for the proof of Lemma 10.

APPENDIX II: PROOFS FOR SECTION IV

This appendix contains the proofs of the Lemmas 7 and 8 regarding the lookup table size reduction techniques described in Section IV. Lemma 11 at the end of the appendix is required by the other lemmas.

Lemma 7: Group index is a one-to-one mapping from the groups of degree n to an integral value between 0 and $n! - 1$.

Proof: As $p_j \geq 0$ for all j , it is obvious that any group index $k \geq 0$. In addition, by the fact that $p_j \leq j - 1$ for all j and Lemma 11 with $i = 1$, it is easy to prove that $k \leq n! - 1$.

For any two different groups, assume the corresponding modified position sequences to be $p_1 p_2 \dots p_n$ and $p'_1 p'_2 \dots p'_n$, and the corresponding group indexes be k and k' , respectively. Since the groups and hence the position sequences are different, the modified sequences should also be different. Let i be the smallest index such that $p_i \neq p'_i$. Without loss of generality, assume $p_i > p'_i$.

$$\begin{aligned}
 k - k' &= \frac{n!}{i!} \times (p_i - p'_i) + \prod_{j=i+1}^n \frac{n!}{j!} \times (p_j - p'_j) \\
 &\geq \frac{n!}{i!} + \prod_{j=i+1}^n \frac{n!}{j!} \times (p_j - p'_j) \\
 &\geq \frac{n!}{i!} - \prod_{j=i+1}^n \frac{n!}{j!} \times (j - 1) \\
 &= \frac{n!}{i!} - \left(\frac{n!}{i!} - 1\right) \text{ by Lemma 11} \\
 &= 1
 \end{aligned}$$

So $k \neq k'$. In other words, different groups will have different group indexes.

Since there are $n!$ groups and each group is mapped to a different integer between 0 and $n! - 1$, the lemma is proved. ■

Lemma 8: Any group of degree n is equivalent to a group with group index between 0 and $n!/4 - 1$.

Proof: For simplicity, we call a group with group index k as group k . For any group k with $k \geq n!/4$, assume the position sequence is $s_1 s_2 \dots s_n$ and the modified position sequence is $p_1 p_2 \dots p_n$. Consider three cases:

- *Case 1)* $3n!/4 \leq k < n!$.

For the group k' that is horizontally symmetrical to group

k , assume the position sequence is $s'_1 s'_2 \dots s'_n$ and the modified position sequence is $p'_1 p'_2 \dots p'_n$. It is clear that $s'_j = n + 1 - s_j$ for $1 \leq j \leq n$. So it follows from the definition of modified position sequence that $p'_j = j - 1 - p_j$ for $1 \leq j \leq n$. Thus,

$$\begin{aligned} k' &= \prod_{j=1}^n \frac{n!}{j!} \times p'_j \\ &= \prod_{j=1}^n \frac{n!}{j!} \times (j - 1 - p_j) \\ &= \prod_{j=1}^n \frac{n!}{j!} \times (j - 1) - k \\ &= n! - 1 - k \quad \text{by Lemma 11} \end{aligned}$$

So $0 \leq k' \leq n!/4 - 1$.

- Case 2) $n!/2 \leq k < 3n!/4$.

As $k \geq n!/2$, p_2 should be 1, which implies $s_1 < s_2$ as shown in Figure 20(a). Consider the group k' in Figure 20(b) which is the same as group k in Figure 20(a) except the relative position of the bottom two pins. Group k and group k' are equivalent due to boundary compaction. For group k' , assume the position sequence is $s'_1 s'_2 \dots s'_n$ and the modified position sequence is $p'_1 p'_2 \dots p'_n$. Then $s'_1 > s'_2$, which implies $p'_2 = 0$. $p_j = p'_j$ for all $j \neq 2$. Therefore, $k' = k - n!/2$. So $0 \leq k' \leq n!/4 - 1$.

- Case 3) $n!/4 \leq k < n!/2$.

We can use the same argument as Case 1 to prove that group k is equivalent to group $k'' = n! - 1 - k$. Therefore, $n!/2 \leq k'' < 3n!/4$. Then we can use the same argument as Case 2 to prove that group k'' (i.e., group k) is equivalent to group $k' = k'' - n!/2$. So $0 \leq k' \leq n!/4 - 1$.

Group k' is between 0 and $n!/4 - 1$ in all cases. Hence, the lemma is proved. ■

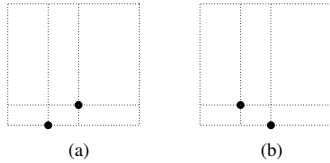


Fig. 20. Relative position of the bottom boundary pins for two equivalent groups.

Lemma 11: For any i such that $1 \leq i \leq n$,

$$\prod_{j=i}^n \frac{n!}{j!} \times (j - 1) = \frac{n!}{(i - 1)!} - 1$$

Proof: The lemma can be proved by induction on i . If $i = n$, both sides equal $n - 1$. Assume $\prod_{j=i}^n \frac{n!}{j!} \times (j - 1) = \frac{n!}{(i - 1)!} - 1$ for some i .

$$\begin{aligned} &\prod_{j=i-1}^n \frac{n!}{j!} \times (j - 1) \\ &= \frac{n!}{(i - 1)!} \times (i - 2) + \prod_{j=i}^n \frac{n!}{j!} \times (j - 1) \end{aligned}$$

$$\begin{aligned} &= \frac{n!}{(i - 1)!} \times (i - 2) + \frac{n!}{(i - 1)!} - 1 \\ &= \frac{n!}{(i - 1)!} \times (i - 1) - 1 \\ &= \frac{n!}{(i - 2)!} - 1 \end{aligned}$$

Hence, the lemma is proved. ■

ACKNOWLEDGMENT

We thank Prof. C. K. Cheng for providing the source code of RST-T and Prof. Hai Zhou for providing the source code of SPAN.

REFERENCES

- [1] M. R. Garey and D. S. Johnson. *Computers and Intractability: A Guide to the Theory of NP-Completeness*. Freeman, NY, 1979.
- [2] F. K. Hwang. On Steiner minimal trees with rectilinear distance. *SIAM Journal of Applied Mathematics*, 30:104–114, 1976.
- [3] F. K. Hwang, D. S. Richards, and P. Winter. The Steiner tree problem. *Annals of Discrete Mathematics*, 1992. Elsevier Science Publishers.
- [4] D. M. Warme, P. Winter, and M. Zachariasen. Exact algorithms for plane Steiner tree problems: A computational study. In D.Z. Du, J.M. Smith, and J.H. Rubinstein, editors, *Advances in Steiner Trees*, pages 81–116. Kluwer Academic Publishers, 2000.
- [5] GeoSteiner – software for computing Steiner trees. <http://www.diku.dk/geosteiner/>.
- [6] J. Griffith, G. Robins, J. S. Salowe, and T. Zhang. Closing the gap: Near-optimal Steiner trees in polynomial time. *IEEE Trans. Computer-Aided Design*, 13(11):1351–1365, November 1994.
- [7] I. I. Mandoiu, V. V. Vazirani, and J. L. Ganley. A new heuristic for rectilinear Steiner trees. In *Proc. IEEE/ACM Intl. Conf. on Computer-Aided Design*, pages 157–162, 1999.
- [8] M. Borah, R. M. Owens, and M. J. Irwin. An edge-based heuristic for Steiner routing. *IEEE Trans. Computer-Aided Design*, 13(12):1563–1568, December 1994.
- [9] Hai Zhou. Efficient Steiner tree construction based on spanning graphs. In *Proc. Intl. Symp. on Physical Design*, pages 152–157, 2003.
- [10] H. Zhou, N. Shenoy, and W. Nicholls. Efficient spanning tree construction without Delaunay triangulation. *Information Processing Letters*, 81(5), 2002.
- [11] A. Kahng, I. Mandoiu, and A. Zelikovsky. Highly scalable algorithms for rectilinear and octilinear Steiner trees. In *Proc. Asian and South Pacific Design Automation Conf.*, pages 827–833, 2003.
- [12] J. Soukup. Circuit layout. *Proceedings of IEEE*, 69:1281–1304, October 1981.
- [13] H. Chen, C. Qiao, F. Zhou, and C.-K. Cheng. Refined single trunk tree: A rectilinear Steiner tree generator for interconnect prediction. In *Proc. ACM Intl. Workshop on System Level Interconnect Prediction*, pages 85–89, 2002.
- [14] C. J. Alpert. The ISPD98 Circuit Benchmark Suite. In *Proc. Intl. Symp. on Physical Design*, pages 80–85, 1998. <http://vlsicad.ucsd.edu/UCLAWeb/cheese/ispd98.html>.
- [15] Andrew B. Kahng and Ion Mandoiu. RMST-Pack: Rectilinear minimum spanning tree algorithms. <http://vlsicad.ucsd.edu/GSRC/bookshelf/Slots/RMST/RMST/>.
- [16] M. Hanan. On Steiner's problem with rectilinear distance. *SIAM Journal of Applied Mathematics*, 14:255–265, 1966.
- [17] Chris Chu. FLUTE: Fast lookup table based technique for RSMT construction and wirelength estimation. <http://vlsicad.ucsd.edu/GSRC/bookshelf/Slots/RMST/>.
- [18] Chris Chu. FLUTE: Fast lookup table based wirelength estimation technique. In *Proc. IEEE/ACM Intl. Conf. on Computer-Aided Design*, pages 696–701, 2004.
- [19] Chris Chu and Yiu-Chung Wong. Fast and accurate rectilinear Steiner minimal tree algorithm for VLSI design. In *Proc. Intl. Symp. on Physical Design*, pages 28–35, 2005.
- [20] A. E. Caldwell, A. B. Kahng, and I. L. Markov. Toward CAD-IP reuse: The MARCO GSRC bookshelf of fundamental CAD algorithms. In *IEEE Design and Test*, pages 72–81, 2002.
- [21] Natarajan Viswanathan and Chris Chu. FastPlace: Efficient analytical placement using cell shifting, iterative local refinement and a hybrid net model. In *Proc. Intl. Symp. on Physical Design*, pages 26–33, 2004.